





Hyperfine structure of the $EF^1\Sigma_g^+$ state in H_2

Hubert Jóźwiak ^{1,*}, Hubert Cybulski ², Antoni Grabowski ¹ and Piotr Wcisło ¹

¹*Institute of Physics, Faculty of Physics, Astronomy and Informatics,*

Nicolaus Copernicus University in Torun, Grudziadzka 5, 87-100 Torun, Poland

²*Institute of Physics, Kazimierz Wielki University, ul. Powstańców Wielkopolskich 2, 85-090 Bydgoszcz, Poland*



(Received 27 May 2021; accepted 28 June 2021; published 16 July 2021)

Calculations of hyperfine splittings in H_2 are needed for an accurate experimental determination of frequencies of rovibrational transitions and the dissociation energy in H_2 , which are used for experimental tests of quantum electrodynamics for molecules and for searches for new physics beyond the standard model. While the hyperfine structure of the ground electronic $X^1\Sigma_g^+$ state in H_2 has been studied in detail, there are no theoretical or experimental data regarding the excited electronic $^1\Sigma_g^+$ states. Here, we report the first investigation of the hyperfine structure of rovibrational levels in the excited double-well $EF^1\Sigma_g^+$ state in the hydrogen molecule. We provide hyperfine splittings and coupling constants for several low-lying rovibrational levels. The hyperfine splittings in the inner well are approximately 1 order of magnitude larger than those in the outer well and 2 times smaller than those in the ground electronic state.

DOI: [10.1103/PhysRevA.104.012808](https://doi.org/10.1103/PhysRevA.104.012808)

I. INTRODUCTION

The hydrogen molecule, the simplest neutral chemically bound system, constitutes a perfect benchmark system for testing *ab initio* quantum-mechanical calculations. Its ground electronic $X^1\Sigma_g^+$ state has been a subject of extensive experimental and theoretical studies for almost a century [1]. Studies of the ionization and dissociation energies [2–9] and the rovibrational structure [10–19] have already achieved a sub-MHz accuracy. An accurate comparison between experimental results and theoretical predictions allows for tests of quantum electrodynamics for molecules [9,10,13]. It can also be used in searches for physics beyond the standard model [20] by putting constraints on hypothetical new forces [21] or higher dimensions [22]. Improvement in the accuracy of calculated and measured dissociation energies and frequencies of rovibrational transitions in the hydrogen molecule would also yield an independent determination of the proton-charge radius or the electron-to-proton mass ratio [10,23,24]. Thus, spectroscopy of molecular hydrogen could complement the accurate studies of the hydrogen molecular ion, which has recently led to the determination of the proton-to-electron mass ratio with a parts-per-trillion relative uncertainty [25,26].

In terms of the excited electronic states of H_2 , particular attention has been paid to the double-well $EF^1\Sigma_g^+$ state, which is the first excited singlet state of the *gerade* symmetry. On the theoretical side, the state was studied extensively by *ab initio* methods [27–35]. Very recently, Siłkowski *et al.* [36] published a set of state-of-the-art Born-Oppenheimer (BO) potential energy curves for several excited electronic $n\Sigma^+$ states (up to $n = 7$), for both singlet and triplet states and the *gerade* and *ungerade* symmetries. The authors reached a relative accuracy of 10^{-10} , improving the previous most

accurate results (see Refs. [33,34] for the $EF^1\Sigma_g^+$ state) by 6 orders of magnitude. On the experimental side, the EF state has been used as an intermediate state in multiphoton transitions, which are used to determine the dissociation energy of *para*- and *ortho*- H_2 . As discussed in Refs. [3,6–8], the dissociation energy of H_2 can be determined from a multistep thermodynamic cycle, which involves the ionization of H_2 , the dissociation of hydrogen ion (H_2^+) and the ionization of atomic hydrogen. The ionization energy of H_2 can be obtained from a series of experiments, which involve the measurement of the energy of a two-photon transition to the inner (E) well of the EF state, the measurement of the energy interval from the E ($\nu = 0, N = 1$) state to one of the highly excited Rydberg states, and the extrapolation to the ionization energy of H_2 , using the multichannel quantum defect theory (MQDT). We note that this sequence can involve either the ground vibrational level of the inner well of the EF state [3,6,8] or the ground vibrational level from the inner (G) well from the next double-well $GK^1\Sigma_g^+$ electronic state [7]. Similar multistep experiments involving the two-photon transition to the excited electronic states were used to determine the energy interval between the first two vibrational states, ($\nu = 0, N = 0$) and ($\nu = 1, N = 0$) [37], and the energy interval between the ground states of *ortho*- and *para*- H_2 [15].

The bound states of the outer (F) well of the EF state are used as intermediate states in the experimental studies of highly excited ($\nu = 11$ –14) vibrational levels of the ground electronic state [38–41]. Two-photon spectroscopy of the F - X transition offers a perfect way to test *ab initio* calculations for these highly excited levels in the ground electronic state. It might also be used in studies of the exotic ($\nu = 14, N = 4$) state, which is speculated to be rotationally predissociative [42], bound by the nonadiabatic effects [10], or a quasibound state that exists due to hyperfine interactions [43].

A remarkable accuracy of both theoretical and experimental studies of the ground electronic state of H_2 and

*hubert.jozwiak@doktorant.umk.pl

its isotopologues has recently driven an increased interest in the underlying hyperfine structure of the rovibrational levels [44–51]. On the one hand, accurate spectroscopy of the molecular hydrogen ion [25] stimulated a parallel progress in the analysis of the hyperfine structure of the H_2^+ , HD^+ [52,53], and D_2^+ ions [54]. On the other hand, there are no available experimental or theoretical data on the hyperfine structure of the excited states of neutral molecular hydrogen. A lack of knowledge about the underlying hyperfine structure of the $(\nu = 0, N = 1)$ level in the inner well of the EF state is one of the factors limiting the accuracy of the recent experimental determination of the dissociation energy of *ortho*- H_2 [8]. This quantity was retrieved from the three-step sequence (*vide supra*) which involved a two-photon excitation from the $(\nu = 0, N = 1) X^1\Sigma_g^+$ state to the $(\nu = 0, N = 1) EF^1\Sigma_g^+$ state, a subsequent two-photon excitation to the $54p1_1$ Rydberg state, and the determination of the ionization energy of the hydrogen molecule from the MQDT. As pointed out by the authors, while the hyperfine structure of the $(\nu = 0, N = 1) X^1\Sigma_g^+$ state could be estimated from the paper of Ramsey [55] and the hyperfine structure of the Rydberg $54p1_1$ state was known from the combination of millimeter spectroscopy and MQDT [56,57], the influence of hyperfine interactions on the structure of the first double-well state has remained unknown.

Here we report the hyperfine structure of rovibrational levels in the excited $EF^1\Sigma_g^+$ state of the hydrogen molecule. Following our previous papers [45–49], we analyze the leading hyperfine interactions in H_2 , we report the spin-rotation coefficient for the EF state, and we provide the hyperfine splittings of the first three rotational states of the *ortho*- H_2 ($N = 1, 3, \text{ and } 5$) from the first seven ($\nu = 0\text{--}6$) vibrational levels, which lie below the barrier that separates the inner and outer wells of the EF state. In Sec. II, we provide some basic information about the excited EF state and rovibrational levels considered in this work. In Sec. III, we recall the information about the hyperfine interactions in H_2 and we provide formulas for the matrix elements of the effective hyperfine Hamiltonian. In Sec. IV, we report a list of rovibrationally averaged spin-rotation and dipole-dipole coupling constants for the 21 states in H_2 . The hyperfine splittings are discussed in Sec. V, where we compare the structure of the first rotational states of the first vibrational states from the E and F wells of the excited state with the splitting of the first rovibrational level in the $X^1\Sigma_g^+$ state. In Sec. VI, we conclude our results.

II. $EF^1\Sigma_g^+$ STATE IN H_2

The $EF^1\Sigma_g^+$ state is the first excited singlet state of the *gerade* manifold, which involves two minima separated by a barrier of approximately 6700 cm^{-1} . The characteristic double-well structure originates from the avoided crossing of two diabatic E and F states [58]. As the internuclear distance tends to infinity, the $EF^1\Sigma_g^+$ state dissociates into the $\text{H}(1s)$ and $\text{H}(2s)$ states. Due to a significant height of the barrier, the lowest bound states in the inner and outer wells behave like for two separated E and F states. This is the reason for the often used distinct labeling system for the states from the E and F wells [59]. The vibrational spacing and the rotational

constant for the states in the E well (approximately 2330 and 63 cm^{-1} , respectively) are significantly larger than the corresponding values in the F well (approximately 1195 and 12 cm^{-1} , respectively) [59].

According to Ref. [30], the $EF^1\Sigma_g^+$ state involves vibrational levels up to $\nu = 33$. We note that states as high as $\nu = 32$ were observed [60,61]. However, as both ν and N increase, the assignment of the levels from the experimental spectra becomes difficult and might lead to some ambiguities [59,62]. Here, we focus on the seven vibrational states which lie below the barrier that separates the E and F wells and we study the hyperfine structure of the first three rotational states from each vibrational manifold (see Fig. 1). The rovibrational levels with $N \leq 5$ were studied in detail by Yu and Dressler [32] using *an initio* BO potential energy curve, while adiabatic corrections and nonadiabatic coupling functions were studied by Ross and Jungen using the MQDT [62,63]. We also recall a recent study by Ferenc and Mátyus [35] of the $(\nu = 0, N \leq 5)$ states from the inner well, where the EF states were obtained as resonances within the four-body problem. Energy intervals between the states considered in this work were also studied experimentally [40,59,62,64].

Figure 1 presents the structure of the rovibrational levels considered in this paper. The square modulus of each rovibrational wave function is plotted against the BO potential energy curve of the $EF^1\Sigma_g^+$ state [36] summed with the contribution from the centrifugal term, $N(N+1)/2\mu R^2$; μ denotes the reduced mass of the H_2 molecule and R is the internuclear distance. The position of each wave function on the energy scale corresponds to the energy of the rovibrational level. For clarity, the graphical representations of the wave function curves shown in Fig. 1 are restricted to the respective well of the potential, except for the $\nu = 6$ states, where the values of the wave functions are non-negligible also in the outer well. The energy of both inner- and outer-well rovibrational levels increases with N due to the contribution from the centrifugal term. This effect is more significant for the inner well states, as shown in Fig. 1. As a result, for $N > 3$, the energy of the $(\nu = 0, N)$ state is higher than the energy of the $(\nu = 1, N)$ state.

Following other studies of the $EF^1\Sigma_g^+$ state [59,62], we use two labeling systems for the rovibrational levels: a combined numbering of levels in the double-well potential, $EF\nu, N$, and an alternative, separate numbering for the E and F states, $E\nu, N$, and $F\nu, N$, respectively). We note, however, that the combined numbering becomes misleading as N increases: the $EF0/E0, N = 5$ state is of higher energy than the $EF1/F0, N = 5$ state.

III. HYPERFINE INTERACTIONS IN THE H_2 MOLECULE

The hyperfine structure of rovibrational levels in the H_2 molecule originates from two leading hyperfine interactions: nuclear spin-rotation interaction and nuclear dipole-dipole interaction. The former is the interaction of the nuclear magnetic dipoles with the magnetic field that originates from the overall rotation of the molecule (both the electrons and the nuclei) [65] and the latter is the magnetic dipole interaction between the two nuclear magnetic moments. We recall that these two hyperfine interactions can be expressed in terms of

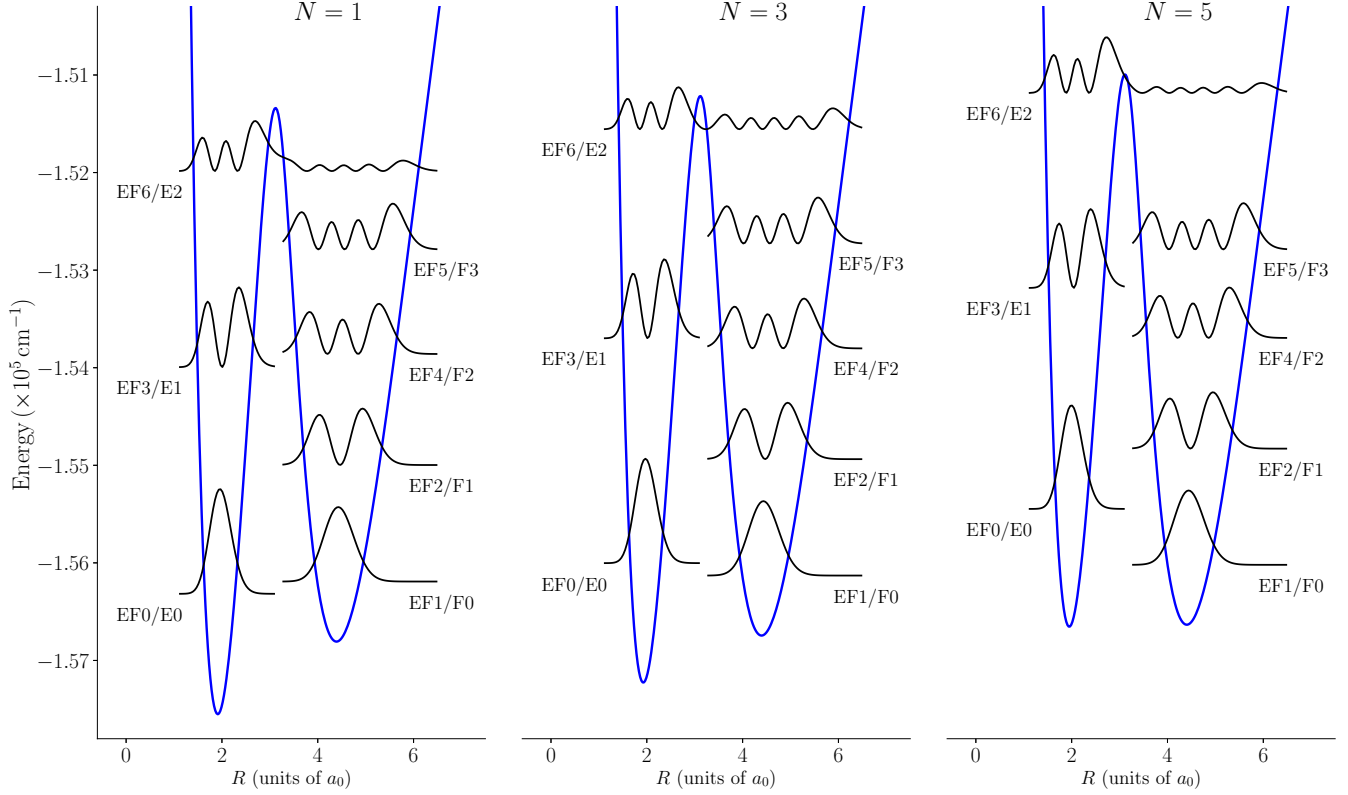


FIG. 1. The square modulus of the $EF^1\Sigma_g^+$ rovibrational ($\nu = 0-6$, $N = 1-5$) wave functions of *ortho*-H₂ considered in this work. The blue (gray) curves represent the potential energy for the $EF^1\Sigma_g^+$ state taken from Ref. [36] with the additional contribution from the centrifugal term for each N .

the three angular momenta: the nuclear spin angular momenta of the two nuclei, \mathbf{I}_1 and \mathbf{I}_2 , and the rotational angular momentum of the nuclei, \mathbf{N} . We construct a coupled basis set out of the three sets of eigenvectors of \mathbf{I}_1^2 , \mathbf{I}_2^2 , and \mathbf{N}^2 . First, we couple the two nuclear spins to form the total nuclear spin angular momentum \mathbf{I} , which, then, is coupled to the rotational angular momentum \mathbf{N} to form the total angular momentum \mathbf{F} . The coupled basis vectors are given as

$$\begin{aligned}
 |\nu; (NI)Fm_F\rangle &= \sum_{m_N=-N}^N \sum_{m_1=-I}^I \langle Nm_N I m_1 | F m_F \rangle \\
 &\quad \times |\nu; Nm_N\rangle |I_1 I_2\rangle |I m_1\rangle \\
 &= \sum_{m_N=-N}^N \sum_{m_1=-I}^I \sum_{m_{11}=-I_1}^{I_1} \sum_{m_{12}=-I_2}^{I_2} \\
 &\quad \times \langle Nm_N I m_1 | F m_F \rangle \langle I_1 m_{11} I_2 m_{12} | I m_1 \rangle \\
 &\quad \times |\nu; Nm_N\rangle |I_1 m_{11}\rangle |I_2 m_{12}\rangle, \quad (1)
 \end{aligned}$$

where $\langle \dots | \dots \rangle$ is a Clebsch-Gordan coefficient; $|I_1 m_{11}\rangle$ and $|I_2 m_{12}\rangle$ are the eigenvectors of \mathbf{I}_1^2 and \mathbf{I}_2^2 , respectively; and $|\nu; Nm_N\rangle = |\nu, N\rangle |Nm_N\rangle$ is a shorthand notation for the rovibrational state, which, in position representation, corresponds to the product of a nuclear wave function (a solution of the nuclear Schrödinger equation in the BO approximation) and a spherical harmonic:

$$\langle \tilde{\mathbf{R}} | \nu; Nm_N \rangle = \chi_{\nu, N}(R) Y_{Nm_N}(\hat{\mathbf{R}}). \quad (2)$$

Here, $\tilde{\mathbf{R}} = (R, \hat{\mathbf{R}})$ is a position vector, which describes the internuclear axis. ν and N denote the vibrational and rotational quantum numbers, respectively.

Following our previous works [45–49], we construct an effective hyperfine Hamiltonian, $\mathcal{H}_{\text{H}_2}^{\text{HF}}$, which involves the two leading hyperfine interactions: the nuclear dipole-dipole interaction and the nuclear spin-rotation interaction:

$$\mathcal{H}_{\text{H}_2}^{\text{HF}} = \mathcal{H}_{\text{dip}} + \mathcal{H}_{\text{nsr}}. \quad (3)$$

We refer the reader to our previous paper regarding the hyperfine structure of rovibrational levels in the $X^1\Sigma_g^+$ state of H₂, where the form of each term in the effective Hamiltonian [46] is discussed. Here, we only write the forms of the leading hyperfine interactions using spherical tensor operators [66,67], and we recall the formulas for the matrix elements of the hyperfine Hamiltonian in the coupled basis.

The nuclear dipole-dipole interaction can be represented as a scalar product of two spherical tensors of rank 2 [67]:

$$\mathcal{H}_{\text{dip}} = -g_1 g_2 \mu_N^2 \frac{\mu_0}{4\pi} \sqrt{6} T^{(2)}(\mathbf{C}) \cdot T^{(1,1,2)}(\mathbf{I}_1, \mathbf{I}_2), \quad (4)$$

where $T^{(2)}(\mathbf{C})$ is the rank-2 spherical tensor corresponding to the spherical harmonic associated with the transformation of the molecular wave function from the laboratory-fixed to the molecule-fixed frame of reference. $T^{(1,1,2)}(\mathbf{I}_1, \mathbf{I}_2)$ is a spherical tensor resulting from the coupling of two spherical tensors of rank 1, $T^{(1)}(\mathbf{I}_1)$ and $T^{(1)}(\mathbf{I}_2)$, which describe the two nuclear spins. $g_1 = g_2 = g_{\text{H}}$ is the g factor of the proton, μ_N is the nuclear magneton, and μ_0 is the vacuum permeability.

TABLE I. Rovibrationally averaged nuclear dipole-dipole coupling constants $c_{\text{dip}}^{v,N}$ (in kHz) for several lowest rovibrational levels in the $EF^1\Sigma_g^+$ state. The estimated relative uncertainty of the data reported here is of an order of 10^{-3} .

N	$EF0/E0$ $\nu = 0$	$EF1/F0$ $\nu = 1$	$EF2/F1$ $\nu = 2$	$EF3/E1$ $\nu = 3$	$EF4/F2$ $\nu = 4$	$EF5/F3$ $\nu = 5$	$EF6/E2$ $\nu = 6$
1	112.87	9.500	9.370	105.45	9.964	10.055	69.07
3	110.56	9.470	9.337	102.66	10.259	9.857	59.82
5	106.56	9.418	9.277	99.17	9.258	9.771	71.85

Matrix elements of the dipole-dipole interaction in a $^1\Sigma$ state are given as

$$\begin{aligned}
& \langle \nu'; (N'(I'_1 I'_2) I') F' m'_F | \mathcal{H}_{\text{dip}} | \nu; (N(I_1 I_2) I) F m_F \rangle \\
&= -\delta_{\nu\nu'} \delta_{F'F} \delta_{m'_F m_F} \delta_{I'_1 I_1} \delta_{I'_2 I_2} \\
& \times c_{\text{dip}}^{v,N} \sqrt{30} (-1)^{N+N'+I'+F'} \\
& \times \begin{pmatrix} N' & 2 & N \\ 0 & 0 & 0 \end{pmatrix} \begin{Bmatrix} N' & N & 2 \\ I & I' & F' \end{Bmatrix} \begin{Bmatrix} I_1 & I_1 & 1 \\ I_2 & I_2 & 1 \\ I' & I & 2 \end{Bmatrix} \\
& \times \sqrt{(2N+1)(2N'+1)(2I'+1)(2I+1)} \\
& \times \sqrt{I_1(I_1+1)(2I_1+1)I_2(I_2+1)(2I_2+1)}, \quad (5)
\end{aligned}$$

where the coupling constant is given as

$$c_{\text{dip}}^{v,N} = g_H^2 \mu_N^2 \frac{\mu_0}{4\pi} \int dR |\chi_{v,N}(R)|^2 R^{-3}. \quad (6)$$

The nuclear spin-rotation term can be represented as a scalar product of spherical tensors of rank 1¹:

$$\mathcal{H}_{\text{nsr}} = -c_{\text{nsr}}(R) T^{(1)}(\mathbf{I}) \cdot T^{(1)}(\mathbf{N}), \quad (7)$$

which describe the total nuclear spin and the nuclear angular momentum, respectively. The strength of the spin-rotation interaction is determined by the nuclear spin-rotation coefficient $c_{\text{nsr}}(R)$, which involves the contributions to the molecular magnetic field from both the electrons and the nuclei, and is a function of the internuclear distance R . Matrix elements of the spin-rotation interaction are obtained using spherical tensor algebra [67]:

$$\begin{aligned}
& \langle \nu'; (N' I') F' m'_F | \mathcal{H}_{\text{nsr}} | \nu; (N I) F m_F \rangle \\
&= -\delta_{F'F} \delta_{m'_F m_F} \delta_{I' I} \delta_{N' N} \frac{c_{\text{nsr}}^{v,N}}{2} \\
& \times [F(F+1) - I(I+1) - N(N+1)]. \quad (8)
\end{aligned}$$

Here, $c_{\text{nsr}}^{v,N}$ is the rovibrationally averaged spin-rotation coefficient:

$$c_{\text{nsr}}^{v,N} = \int dR |\chi_{v,N}(R)|^2 c_{\text{nsr}}(R). \quad (9)$$

The effective Hamiltonian is, thus, diagonal with respect to the total angular momentum F and its projection on the space-fixed Z axis, m_F . The dipole-dipole interaction introduces a weak coupling between different rotational states, $N' = N \pm 2$. However, these off-diagonal terms in the hyperfine Hamiltonian are approximately 10 orders of magnitude smaller than the energy difference between rovibrational levels. This allows us to neglect any possible coupling between different rotational states. In such a case, the coupled basis vectors constitute the eigenbasis of the effective hyperfine Hamiltonian, and the hyperfine splittings of the rovibrational levels are obtained immediately.

IV. HYPERFINE COUPLING CONSTANTS IN THE $EF^1\Sigma_g^+$ STATE

The magnitude of hyperfine splittings of each rovibrational level is determined by the hyperfine coupling constants. The nuclear dipole-dipole coupling constant depends only on the g factors of the nuclei, the nuclear magneton, and the average over the expectation value of the $1/R^3$ term in a given rovibrational state. Here, we employ the values of g_H , μ_0 , and μ_N recommended by CODATA [68]. The $\chi_{v,N}(R)$ wave functions for each rovibrational state were obtained by solving the nuclear Schrödinger equation in the BO approximation using the finite basis discrete variable representation method [69] implemented in the BIGOS package [70]. The calculations were performed for internuclear distances in a range of 0.7–20.0 a_0 with steps of 0.04 a_0 . We used the recently published BO potential energy curve for the $EF^1\Sigma_g^+$ state [36]. The uncertainty of the nuclear dipole-dipole coupling constants originates from the neglected nonadiabatic effects, which are of an order of the ratio of the electron mass to the reduced mass of H_2 [51]. The obtained coefficients are listed in Table I. We observe a significant difference between the obtained nuclear dipole-dipole coupling constants for the states from the inner well and the outer well—the former are 1 order of magnitude larger than the latter. This is due to the fact that the expectation values of the $1/R^3$ term are clearly greater for the states from the inner well. We also note that the nuclear dipole-dipole coupling coefficients for the states from the E well of the potential exhibit a more significant dependence on the rotational quantum number and that they are approximately 2 times smaller than those of the first rovibrational levels of the $X^1\Sigma_g^+$ state (see Table 1 in Ref. [46]). As ν increases, the values of the nuclear dipole-dipole coupling constants for the states from the E well decrease, while those for the F well states increase.

¹We note that in our previous papers [45–47], the sign of the spin-rotation term in the effective Hamiltonian was incorrect.

TABLE II. Rovibrationally averaged nuclear spin-rotation constants $c_{\text{nsr}}^{v,N}$ (in kHz) for the several low-lying rovibrational levels in the $EF^1\Sigma_g^+$ state.

N	$EF0/E0$ $\nu = 0$	$EF1/F0$ $\nu = 1$	$EF2/F1$ $\nu = 2$	$EF3/E1$ $\nu = 3$	$EF4/F2$ $\nu = 4$	$EF5/F3$ $\nu = 5$	$EF6/E2$ $\nu = 6$
1	47.37	-11.44	-11.53	44.40	-11.20	-11.29	23.06
3	46.23	-11.39	-11.47	42.99	-10.98	-11.29	19.19
5	44.28	-11.30	-11.38	41.23	-11.41	-11.15	25.93

Nuclear spin-rotation constants were calculated at the full configuration-interaction level using London orbitals [71]. The double-augmented d-aug-cc-pVQZ basis set [72] was used. The calculations were performed for the internuclear R distances in the 0.98–24.40 a_0 range mostly with steps of 0.04 a_0 . The numerical results of the R -dependent coupling constants are provided in the Supplemental Material [73]. All the calculations have been performed with Dalton, a molecular electronic structure program, Release v2020.0.beta, [74].

The convergence of the spin-rotation coupling constants with the basis set size can be estimated solely by a comparison of the d-aug-cc-pVTZ and d-aug-cc-pVQZ results. In the double-well region the spin-rotation coupling constants are 50.502 and 50.379 kHz (at $R = 1.89 a_0$) or -11.763 and -11.868 kHz (at $R = 4.35 a_0$) calculated with the d-aug-cc-pVTZ basis set and the d-aug-cc-pVQZ basis set, respectively. For the errors emerging from neglect of the relativistic effects, contributions beyond the Born-Oppenheimer approximation, and inaccuracies in the used potential curve, we can use the estimate of 200 Hz, which we have quoted previously [45] for the ground state of the hydrogen molecule (see Refs. [75,76] and cf. Ref. [44]). This gives the total uncertainty of the calculated spin-rotation constants at a level of ca. 350 Hz.

We note here, that the nonadiabatic contributions to the calculated $c_{\text{nsr}}^{v,N}$ are expected to be included within the estimated uncertainty, since the low-lying rovibrational levels considered here are predominantly of the EF character (the probability of finding the EF electronic state in a given nonadiabatic rovibronic state is larger than 0.999 37) [32]. Moreover, the nonadiabatic corrections [32] to the adiabatic variational term values reported in Ref. [30] for the ($\nu = 0-6$, $N = 0$) levels are, at most, 0.007%. By contrast, the nonadiabatic effects are more pronounced in the low-lying levels of the $GK^1\Sigma_g^+$ state. For instance, the probabilities of finding the EF and GK states in the ($\nu = 0$, $N = 1$) nonadiabatic rovibronic state are 0.399 69 and 0.583 68, respectively [32].

Rovibrationally averaged spin-rotation coupling constants are listed in Table II. Similarly as in the case of the nuclear dipole-dipole interaction, we observe a significant difference between the coupling constants for the inner and outer well levels. The nuclear spin-rotation couplings for the E -well states are positive and approximately 2.5 times smaller than those calculated for the ground electronic state [46]. Conversely, the constants for the F -well states are negative and of the order of the nuclear dipole-dipole coupling coefficients. This is due to the fact that the rovibrational average [Eq. (6)] probes the long-range part of the $c_{\text{nsr}}(R)$, where the nuclear spin-rotation coupling is negative [see Fig. 2(b)]. The difference between the E and F states becomes less pronounced for larger values of ν .

V. HYPERFINE SPLITTINGS OF ROVIBRATIONAL LEVELS IN THE $EF^1\Sigma_g^+$ STATE

We have calculated hyperfine splittings for several low-lying rovibrational levels of the $EF^1\Sigma_g^+$ state in H_2 . We studied the three lowest rotational levels in the first seven vibrational states, which lie below the barrier that separates the two minima on the BO potential energy curve. Following the discussion in the previous section, we estimate the uncertainty of determined hyperfine energy levels to be approximately 0.35 kHz, if not less. A complete table containing the values of the energies of the hyperfine levels is provided in the Supplemental Material [73].

In this section, we discuss an example of the hyperfine splittings in the first two rovibrational levels of *ortho*- H_2 , i.e., $EF0/E0$, $N = 1$ and $EF1/F0$, $N = 1$, from the inner and outer wells of the BO potential energy curve. Moreover, we compare the hyperfine splittings with the ($\nu = 0$, $N = 1$) level of the ground $X^1\Sigma_g^+$ electronic state (see Fig. 2), analyzed in previous papers [46,49]. We recall that the vibrationally averaged nuclear spin-rotation constant and the nuclear dipole-dipole constant for this level are $c_{\text{nsr}}^{v,N} = 114.16$ kHz and $c_{\text{dip}}^{v,N} = 288.22$ kHz, respectively [46].

The first rotational state is split into three hyperfine states with $F = 0, 1$, and 2. The energy of each state is given as

$$\begin{aligned}
 E_{\nu,N=1,F} &= (-1)^F 3c_{\text{dip}}^{v,N} \begin{Bmatrix} 1 & 1 & 2 \\ 1 & 1 & F \end{Bmatrix} \\
 &\quad - \frac{c_{\text{nsr}}^{v,N}}{2} [F(F+1) - 4] \\
 &= \begin{cases} c_{\text{dip}}^{v,N} + 2c_{\text{nsr}}^{v,N} & \text{if } F = 0, \\ -\frac{1}{2}c_{\text{dip}}^{v,N} + c_{\text{nsr}}^{v,N} & \text{if } F = 1, \\ \frac{1}{10}c_{\text{dip}}^{v,N} - c_{\text{nsr}}^{v,N} & \text{if } F = 2, \end{cases} \quad (10)
 \end{aligned}$$

which can be verified by a careful examination of Eqs. (5) and (8). The hyperfine splittings of these states are presented in Fig. 2(c). The hyperfine splittings of the $E0$ state are of an order of several hundreds of kHz, quite similar to those of the ground state. In contrast, the splittings in the first vibrational state in the outer well are 1 order of magnitude smaller than those for the inner well. We also note that the ordering of the hyperfine states in this level is different than that observed for the inner well or for the ground electronic state. This follows from the change of the sign of the nuclear spin-rotation coupling and the fact that its absolute value is close to the value of the nuclear dipole-dipole coupling constant [see Fig. 2(b)].

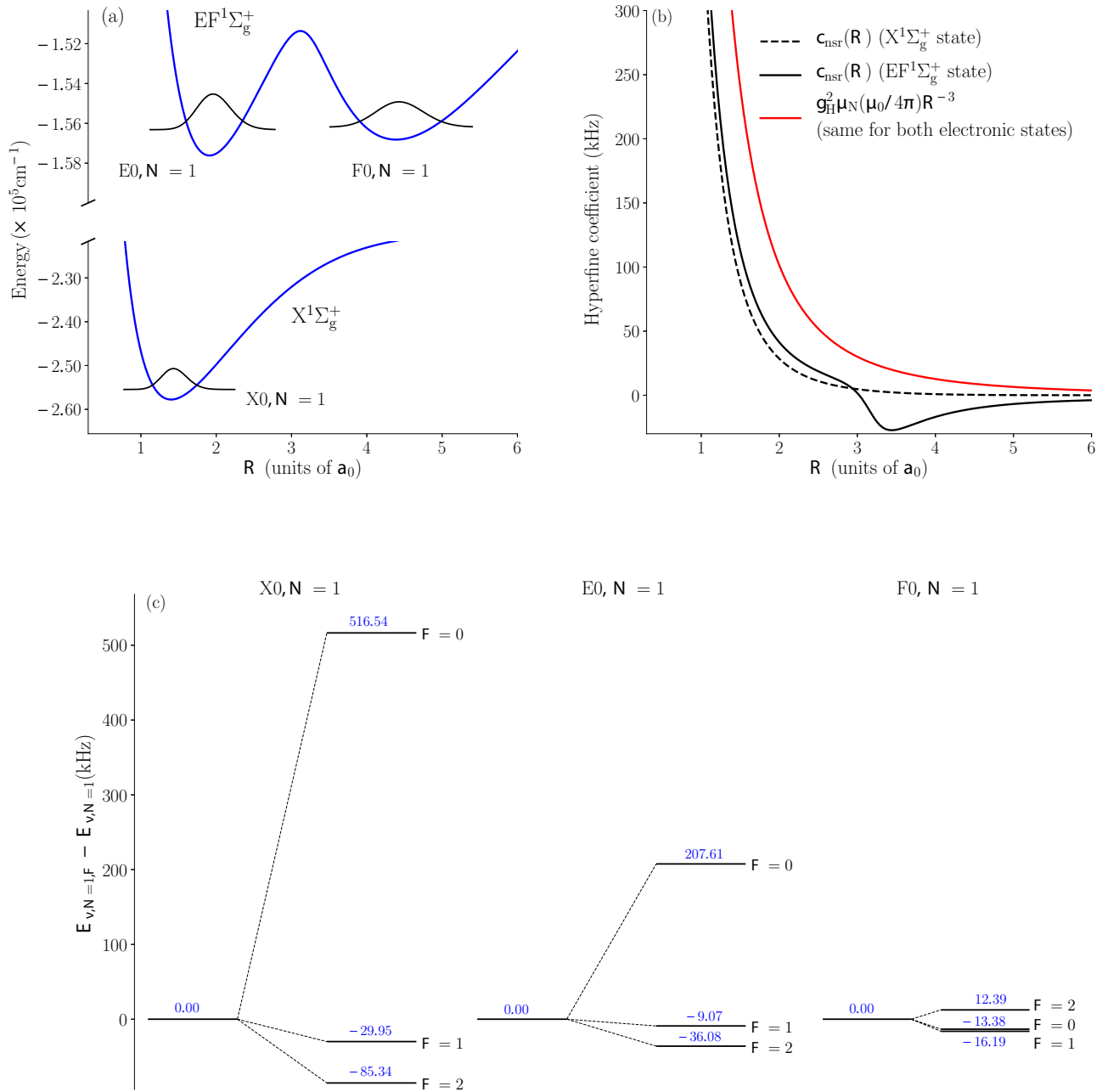


FIG. 2. Hyperfine structure of the first rovibrational levels in *ortho*-H₂ in the $X^1\Sigma_g^+$ state and the *E* and *F* wells of the $EF^1\Sigma_g^+$ state. Panel (a) presents the BO potential energy curves for the two electronic states [36,77] and the wave functions of the three considered rovibrational levels. Panel (b) presents the hyperfine coefficients for the excited states (solid lines) and the ground electronic state (dashed lines). We note that the nuclear dipole-dipole coupling constants are independent of the electronic state. Panel (c) presents a direct comparison between the hyperfine splittings in the three states: the $X^1\Sigma_g^+$ (left) state and the *E* (center) and *F* (right) wells of the $EF^1\Sigma_g^+$ state.

VI. CONCLUSION

We have analyzed the hyperfine structure of the excited double-well $EF^1\Sigma_g^+$ state in the H₂ molecule. Similarly as in the case of the ground electronic state, the hyperfine splittings originate mostly from the nuclear spin-rotation and nuclear dipole-dipole interactions. Hyperfine splitting of the $N=1$ rotational state in the inner well is approximately 2 times smaller than that of the first rotational level in the ground electronic state. Furthermore, the outer-well levels exhibit a

hyperfine structure which is approximately 1 order of magnitude smaller than the one from the inner well. The magnitude of the coupling constants and the resulting hyperfine splittings in the $EF^1\Sigma_g^+$ state decrease as the vibrational and rotational quantum numbers increase.

The results presented here are of significant importance for the ultra-accurate spectroscopies of H₂. Knowledge about the hyperfine structure of the $EF^1\Sigma_g^+$ state would reduce the uncertainty of several physical quantities determined from the

Doppler-free spectroscopy, such as the dissociation energy of *ortho*- H_2 . Improved accuracy of spectroscopic measurements of molecular hydrogen could in turn lead to even more stringent tests of quantum electrodynamics for molecules and physics beyond the standard model. A methodology similar to that presented here can be used to study the $EF^1\Sigma_g^+$ state in the HD and D_2 molecules. However, for these two isotopologues, an additional influence of the interaction between the electric quadrupole moment of the deuteron and the electric field gradient has to be taken into account.

ACKNOWLEDGMENTS

The research is financed from the budgetary funds on science projected for 2019–2023 as a research project under the “Diamantowy Grant” program. P.W. is supported by the National Science Centre in Poland, Project No. 2019/35/B/ST2/01118. Calculations have been carried out using resources provided by the Wrocław Centre for Networking and Supercomputing (see Ref. [78]), Grant No. 294. The research is a part of the program of the National Laboratory FAMO in Toruń, Poland.

-
- [1] D. Sprecher, C. Jungen, W. Ubachs, and F. Merkt, Towards measuring the ionisation and dissociation energies of molecular hydrogen with sub-MHz accuracy, *Faraday Discuss.* **150**, 51 (2011).
- [2] K. Piszczatowski, G. Łach, M. Przybytek, J. Komasa, K. Pachucki, and B. Jeziorski, Theoretical determination of the dissociation energy of molecular hydrogen, *J. Chem. Theory Comput.* **5**, 3039 (2009).
- [3] J. Liu, E. J. Salumbides, U. Hollenstein, J. C. J. Koelemeij, K. S. E. Eikema, W. Ubachs, and F. Merkt, Determination of the ionization and dissociation energies of the hydrogen molecule, *J. Chem. Phys.* **130**, 174306 (2009).
- [4] M. Puchalski, A. Spyszkiwicz, J. Komasa, and K. Pachucki, Nonadiabatic Relativistic Correction to the Dissociation Energy of H_2 , D_2 , and HD, *Phys. Rev. Lett.* **121**, 073001 (2018).
- [5] L. M. Wang and Z.-C. Yan, Relativistic corrections to the ground state of H_2 calculated without using the Born-Oppenheimer approximation, *Phys. Rev. A* **97**, 060501 (2018).
- [6] R. K. Altmann, L. S. Dreissen, E. J. Salumbides, W. Ubachs, and K. S. E. Eikema, Deep-Ultraviolet Frequency Metrology of H_2 for Tests of Molecular Quantum Theory, *Phys. Rev. Lett.* **120**, 043204 (2018).
- [7] C.-F. Cheng, J. Hussels, M. Niu, H. L. Bethlem, K. S. E. Eikema, E. J. Salumbides, W. Ubachs, M. Beyer, N. Hölsch, J. A. Agner, F. Merkt, L.-G. Tao, S.-M. Hu, and C. Jungen, Dissociation Energy of the Hydrogen Molecule at 10^{-9} Accuracy, *Phys. Rev. Lett.* **121**, 013001 (2018).
- [8] N. Hölsch, M. Beyer, E. J. Salumbides, K. S. E. Eikema, W. Ubachs, C. Jungen, and F. Merkt, Benchmarking Theory with an Improved Measurement of the Ionization and Dissociation Energies of H_2 , *Phys. Rev. Lett.* **122**, 103002 (2019).
- [9] M. Puchalski, J. Komasa, P. Czachorowski, and K. Pachucki, Nonadiabatic QED Correction to the Dissociation Energy of the Hydrogen Molecule, *Phys. Rev. Lett.* **122**, 103003 (2019).
- [10] J. Komasa, K. Piszczatowski, G. Łach, M. Przybytek, B. Jeziorski, and K. Pachucki, Quantum electrodynamics effects in rovibrational spectra of molecular hydrogen, *J. Chem. Theory Comput.* **7**, 3105 (2011).
- [11] P. Weislo, F. Thibault, M. Zaborowski, S. Wójtewicz, A. Cygan, G. Kowzan, P. Masłowski, J. Komasa, M. Puchalski, K. Pachucki, R. Ciuryło, and D. Lisak, Accurate deuterium spectroscopy for fundamental studies, *J. Quant. Spectrosc. Radiat. Transfer* **213**, 41 (2018).
- [12] E. Fasci, A. Castrillo, H. Dinesan, S. Gravina, L. Moretti, and L. Gianfrani, Precision spectroscopy of HD at $1.38\ \mu\text{m}$, *Phys. Rev. A* **98**, 022516 (2018).
- [13] J. Komasa, M. Puchalski, P. Czachorowski, G. Łach, and K. Pachucki, Rovibrational energy levels of the hydrogen molecule through nonadiabatic perturbation theory, *Phys. Rev. A* **100**, 032519 (2019).
- [14] M. L. Diouf, F. M. J. Cozijn, B. Darquié, E. J. Salumbides, and W. Ubachs, Lamb-dips and Lamb-peaks in the saturation spectrum of HD, *Opt. Lett.* **44**, 4733 (2019).
- [15] M. Beyer, N. Hölsch, J. Hussels, C.-F. Cheng, E. J. Salumbides, K. S. E. Eikema, W. Ubachs, C. Jungen, and F. Merkt, Determination of the Interval between the Ground States of Para- and Ortho- H_2 , *Phys. Rev. Lett.* **123**, 163002 (2019).
- [16] T.-P. Hua, Y. R. Sun, and S.-M. Hu, Dispersion-like lineshape observed in cavity-enhanced saturation spectroscopy of HD at $1.4\ \mu\text{m}$, *Opt. Lett.* **45**, 4863 (2020).
- [17] M. Zaborowski, M. Słowiński, K. Stankiewicz, F. Thibault, A. Cygan, H. Józwiak, G. Kowzan, P. Masłowski, A. Nishiyama, N. Stolarczyk, S. Wójtewicz, R. Ciuryło, D. Lisak, and P. Weislo, Ultrahigh finesse cavity-enhanced spectroscopy for accurate tests of quantum electrodynamics for molecules, *Opt. Lett.* **45**, 1603 (2020).
- [18] A. Fast and S. A. Meek, Sub-ppb Measurement of a Fundamental Band Rovibrational Transition in HD, *Phys. Rev. Lett.* **125**, 023001 (2020).
- [19] M. L. Diouf, F. M. J. Cozijn, K.-F. Lai, E. J. Salumbides, and W. Ubachs, Lamb-peak spectrum of the HD (2-0) P(1) line, *Phys. Rev. Res.* **2**, 023209 (2020).
- [20] W. Ubachs, J. Koelemeij, K. Eikema, and E. Salumbides, Physics beyond the standard model from hydrogen spectroscopy, *J. Mol. Spectrosc.* **320**, 1 (2016).
- [21] E. J. Salumbides, J. C. J. Koelemeij, J. Komasa, K. Pachucki, K. S. E. Eikema, and W. Ubachs, Bounds on fifth forces from precision measurements on molecules, *Phys. Rev. D* **87**, 112008 (2013).
- [22] E. J. Salumbides, A. N. Schellekens, B. Gato-Rivera, and W. Ubachs, Constraints on extra dimensions from precision molecular spectroscopy, *New J. Phys.* **17**, 033015 (2015).
- [23] M. Puchalski, J. Komasa, P. Czachorowski, and K. Pachucki, Complete $\alpha^6 m$ Corrections to the Ground State of H_2 , *Phys. Rev. Lett.* **117**, 263002 (2016).
- [24] J.-P. Karr, D. Marchand, and E. Voutier, The proton size, *Nat. Rev. Phys.* **2**, 601 (2020).
- [25] S. Patra, M. Germann, J.-P. Karr, M. Haidar, L. Hilico, V. I. Korobov, F. M. J. Cozijn, K. S. E. Eikema, W. Ubachs, and J. C. J. Koelemeij, Proton-electron mass ratio from laser spectroscopy of HD^+ at the part-per-trillion level, *Science* **369**, 1238 (2020).

- [26] S. Alighanbari, G. S. Giri, F. L. Constantin, V. I. Korobov, and S. Schiller, Precise test of quantum electrodynamics and determination of fundamental constants with HD^+ ions, *Nature (London)* **581**, 152 (2020).
- [27] J. Gerhauser and H. S. Taylor, *Ab initio* calculation of the $E^1\Sigma_g^+$ and a $^3\Sigma_g^+$ states of the hydrogen molecule, *J. Chem. Phys.* **42**, 3621 (1965).
- [28] W. Kołos and L. Wolniewicz, Theoretical investigation of the lowest double-minimum state $E, F^1\Sigma_g^+$ of the hydrogen molecule, *J. Chem. Phys.* **50**, 3228 (1969).
- [29] K. Dressler, R. Gallusser, P. Quadrelli, and L. Wolniewicz, The EF and $GK^1\Sigma_g^+$ states of hydrogen, *J. Mol. Spectrosc.* **75**, 205 (1979).
- [30] L. Wolniewicz and K. Dressler, The EF , GK , and $HH^1\Sigma_g^+$ states of hydrogen. Improved *ab initio* calculation of vibrational states in the adiabatic approximation, *J. Chem. Phys.* **82**, 3292 (1985).
- [31] P. Quadrelli, K. Dressler, and L. Wolniewicz, Nonadiabatic coupling between the $EF+GK+H^1\Sigma_g^+, I^1\Pi_g$, and $J^1\Delta_g$ states of the hydrogen molecule. Calculation of rovibronic structures in H_2 , HD , and D_2 , *J. Chem. Phys.* **92**, 7461 (1990).
- [32] S. Yu and K. Dressler, Calculation of rovibronic structures in the lowest nine excited $^1\Sigma_g^+ + ^1\Pi_g + ^1\Delta_g$ states of H_2 , D_2 , and T_2 , *J. Chem. Phys.* **101**, 7692 (1994).
- [33] T. Orlikowski, G. Staszewska, and L. Wolniewicz, Long range adiabatic potentials and scattering lengths for the EF , e and h states of the hydrogen molecule, *Mol. Phys.* **96**, 1445 (1999).
- [34] J. Komasa and C. Wojciech, Exponentially correlated Gaussian functions in variational calculations. The $EF^1\Sigma_g^+$ state of hydrogen molecule, *Comput. Methods Sci. Technol.* **9**, 79 (2003).
- [35] D. Ferenc and E. Mátyus, Computation of rovibronic resonances of molecular hydrogen: $EF^1\Sigma_g^+$ inner-well rotational states, *Phys. Rev. A* **100**, 020501 (2019).
- [36] M. Siłkowski, M. Zientkiewicz, and K. Pachucki, Accurate Born-Oppenheimer potentials for excited Σ^+ states of the hydrogen molecule (2021), [arXiv:2104.03174](https://arxiv.org/abs/2104.03174).
- [37] G. D. Dickenson, M. L. Niu, E. J. Salumbides, J. Komasa, K. S. E. Eikema, K. Pachucki, and W. Ubachs, Fundamental Vibration of Molecular Hydrogen, *Phys. Rev. Lett.* **110**, 193601 (2013).
- [38] M. Niu, E. Salumbides, G. Dickenson, K. Eikema, and W. Ubachs, Precision spectroscopy of the $X^1\Sigma_g^+, v=0 \rightarrow 1(J=0-2)$ rovibrational splittings in H_2 , HD and D_2 , *J. Mol. Spectrosc.* **300**, 44 (2014).
- [39] T. M. Trivikram, M. L. Niu, P. Wcisło, W. Ubachs, and E. J. Salumbides, Precision measurements and test of molecular theory in highly excited vibrational states of H_2 ($v=11$), *Appl. Phys. B* **122**, 294 (2016).
- [40] T. M. Trivikram, E. J. Salumbides, C. Jungen, and W. Ubachs, Excitation of H_2 at large internuclear separation: Outer well states and continuum resonances, *Mol. Phys.* **117**, 2961 (2019).
- [41] K.-F. Lai, M. Beyer, E. J. Salumbides, and W. Ubachs, Photolysis production and spectroscopic investigation of the highest vibrational states in H_2 ($X^1\Sigma_g^+ v=13, 14$), *J. Phys. Chem. A* **125**, 1221 (2021).
- [42] R. J. L. Roy and R. B. Bernstein, Shape resonances and rotationally predissociating levels: The atomic collision time-delay functions and quasibound level properties of $\text{H}_2(X^1\Sigma_g^+)$, *J. Chem. Phys.* **54**, 5114 (1971).
- [43] M. Selg, A quasi-bound rovibrational state of hydrogen molecule resulting from hyperfine proton-electron spin-spin interaction, *Europhys. Lett.* **96**, 10009 (2011).
- [44] P. Dupré, Hyperfine transitions in the first overtone mode of hydrogen deuteride, *Phys. Rev. A* **101**, 022504 (2020).
- [45] H. Józwiak, H. Cybulski, and P. Wcisło, Positions and intensities of hyperfine components of all rovibrational dipole lines in the HD molecule, *J. Quant. Spectrosc. Radiat. Transfer* **253**, 107171 (2020).
- [46] H. Józwiak, H. Cybulski, and P. Wcisło, Hyperfine components of all rovibrational quadrupole transitions in the H_2 and D_2 molecules, *J. Quant. Spectrosc. Radiat. Transfer* **253**, 107186 (2020).
- [47] H. Józwiak, H. Cybulski, and P. Wcisło, Hyperfine structure of quadrupole rovibrational transitions in tritium-bearing hydrogen isotopologues, *J. Quant. Spectrosc. Radiat. Transfer* **256**, 107255 (2020).
- [48] H. Józwiak, H. Cybulski, and P. Wcisło, Hyperfine components of rovibrational dipole transitions in HT and DT , *J. Quant. Spectrosc. Radiat. Transfer* **270**, 107662 (2021).
- [49] H. Józwiak, H. Cybulski, and P. Wcisło, Hyperfine components of rovibrational quadrupole transitions in HD , *J. Quant. Spectrosc. Radiat. Transfer*, **272**, 107753 (2021).
- [50] J. Komasa, M. Puchalski, and K. Pachucki, Hyperfine structure in the HD molecule, *Phys. Rev. A* **102**, 012814 (2020).
- [51] M. Puchalski, J. Komasa, and K. Pachucki, Hyperfine Structure of the First Rotational Level in H_2 , D_2 and HD Molecules and the Deuteron Quadrupole Moment, *Phys. Rev. Lett.* **125**, 253001 (2020).
- [52] J.-P. Karr, M. Haidar, L. Hilico, Z.-X. Zhong, and V. I. Korobov, Higher-order corrections to spin-spin scalar interactions in HD^+ and H_2^+ , *Phys. Rev. A* **102**, 052827 (2020).
- [53] V. I. Korobov, J.-P. Karr, M. Haidar, and Z.-X. Zhong, Hyperfine structure in the H_2^+ and HD^+ molecular ions at order ma^6 , *Phys. Rev. A* **102**, 022804 (2020).
- [54] P. Danev, D. Bakalov, V. I. Korobov, and S. Schiller, Hyperfine structure and electric quadrupole transitions in the deuterium molecular ion, *Phys. Rev. A* **103**, 012805 (2021).
- [55] N. F. Ramsey, Theory of molecular hydrogen and deuterium in magnetic fields, *Phys. Rev.* **85**, 60 (1952).
- [56] A. Osterwalder, A. Wüest, F. Merkt, and C. Jungen, High-resolution millimeter wave spectroscopy and multichannel quantum defect theory of the hyperfine structure in high Rydberg states of molecular hydrogen H_2 , *J. Chem. Phys.* **121**, 11810 (2004).
- [57] D. Sprecher, C. Jungen, and F. Merkt, Determination of the binding energies of the np Rydberg states of H_2 , HD , and D_2 from high-resolution spectroscopic data by multichannel quantum-defect theory, *J. Chem. Phys.* **140**, 104303 (2014).
- [58] E. R. Davidson, First excited $^1\Sigma_g^+$ state of the hydrogen molecule, *J. Chem. Phys.* **35**, 1189 (1961).
- [59] D. Bailly, E. Salumbides, M. Vervloet, and W. Ubachs, Accurate level energies in the $EF^1\Sigma_g^+, GK^1\Sigma_g^+, H^1\Sigma_g^+, B^1\Sigma_u^+, C^1\Pi_u, B^1\Sigma_u^+, D^1\Pi_u, I^1\Pi_g, J^1\Delta_g$ states of H_2 , *Mol. Phys.* **108**, 827 (2010).
- [60] K. Tsukiyama, S. Shimizu, and T. Kasuya, Identification of the $EF^1\Sigma_g^+(v'=31 \text{ and } 32)$ states of H_2 by XUV-VIS double-resonance spectroscopy, *J. Mol. Spectrosc.* **155**, 352 (1992).

- [61] E. Reinhold, A. de Lange, W. Hogervorst, and W. Ubachs, Observation of the $I^1\Pi_g$ outer well state in H_2 and D_2 , *J. Chem. Phys.* **109**, 9772 (1998).
- [62] G. D. Dickenson, E. J. Salumbides, M. Niu, C. Jungen, S. C. Ross, and W. Ubachs, Precision spectroscopy of high rotational states in H_2 investigated by Doppler-free two-photon laser spectroscopy in the $EF^1\Sigma_g^+-X^1\Sigma_g^+$ system, *Phys. Rev. A* **86**, 032502 (2012).
- [63] S. C. Ross and C. Jungen, Multichannel quantum-defect theory of $n = 2$ and 3 gerade states in H_2 : Rovibronic energy levels, *Phys. Rev. A* **50**, 4618 (1994).
- [64] M. S. Quinn, K. Nauta, and S. H. Kable, Disentangling the $H_2E, F(1^1\Sigma_g^+)(v' = 0 - 18) \leftarrow X(1^1\Sigma_g^+)(v'' = 3 - 9)(2 + 1)$ REMPI spectrum via 2D velocity-mapped imaging, *Mol. Phys.* **119**, e1836412 (2021).
- [65] W. H. Flygare, Spin-rotation interaction and magnetic shielding in molecules, *J. Chem. Phys.* **41**, 793 (1964).
- [66] U. Fano and G. Racah, *Irreducible Tensorial Sets* (Academic, New York, 1959).
- [67] J. M. Brown and A. Carrington, *Rotational Spectroscopy of Diatomic Molecules* (Cambridge University, Cambridge, England, 2003).
- [68] See <http://physics.nist.gov/cuu/Constants> for CODATA 2018 recommended values of the fundamental constants (CODATA 2018) (last accessed May, XXth, 2021).
- [69] J. Lill, G. Parker, and J. Light, Discrete variable representations and sudden models in quantum scattering theory, *Chem. Phys. Lett.* **89**, 483 (1982).
- [70] H. Jóźwiak, M. Gancewski, A. Grabowski, K. Stankiewicz, and P. Wcisło, BIGOS computer code, to be published.
- [71] J. Gauss, K. Ruud, and T. Helgaker, Perturbation-dependent atomic orbitals for the calculation of spin-rotation constants and rotational g tensors, *J. Chem. Phys.* **105**, 2804 (1996).
- [72] T. H. Dunning, Jr., Gaussian basis sets for use in correlated molecular calculations. I. The atoms boron through neon and hydrogen, *J. Chem. Phys.* **90**, 1007 (1989).
- [73] H. Jóźwiak, H. Cybulski, and P. Wcisło, See supplemental Material at <http://link.aps.org/supplemental/10.1103/PhysRevA.104.012808> for the hyperfine splittings and hyperfine coupling constants.
- [74] K. Aidas, C. Angeli, K. L. Bak, V. Bakken, R. Bast, L. Boman, O. Christiansen, R. Cimraglia, S. Coriani, P. Dahle, E. K. Dalskov, U. Ekström, T. Enevoldsen, J. J. Eriksen, P. Ettenhuber, B. Fernández, L. Ferrighi, H. Fliegl, L. Frediani, K. Hald *et al.*, The Dalton quantum chemistry program system, *WIREs Comput. Mol. Sci.* **4**, 269 (2014); see also <http://daltonprogram.org>.
- [75] D. Sundholm and J. Gauss, Isotope and temperature effects on nuclear magnetic shieldings and spin-rotation constants calculated at the coupled-cluster level, *Mol. Phys.* **92**, 1007 (1997).
- [76] J. Gauss and D. Sundholm, Coupled-cluster calculations of spin-rotation constants, *Mol. Phys.* **91**, 449 (1997).
- [77] K. Pachucki, Born-Oppenheimer potential for H_2 , *Phys. Rev. A* **82**, 032509 (2010).
- [78] <http://wcss.pl>.